2011 NDIA GROUND VEHICLE SYSTEMS ENGINEERING AND TECHNOLOGY SYMPOSIUM
MODELING & SIMULATION, TESTING AND VALIDATION (MSTV) MINI-SYMPOSIUM
AUGUST 9-11 DEARBORN, MICHIGAN

TACTILE TERRAIN PREDICTION FOR AUTONOMOUS AND TELE-OPERATED GROUND VEHICLES

Dr. Steve Southward
Department of Mechanical Engineering
Virginia Polytechnic Institute and State University
Danville, VA

ABSTRACT

Lidar, Sonar, and Vision-based measurements are often used to preview terrain topology for unmanned ground vehicles. Environmental conditions such as wet or snow-covered roads, shadows, superficial ground coverings, and deceptive surface textures can lead to erroneous measurements. Tactile terrain prediction is both an alternative and a supplement to existing measurement systems. Tactile feedback from an array of low-cost sensors on the moving vehicle is used to generate low wave-number terrain profile predictions. This paper presents tactile terrain prediction results evaluated on four unique courses. Prediction error data are presented up to 25m in front of the vehicle. Results indicate 0.02-0.2m RMS error and 0.18-1.0m peak error at a 10m look-ahead distance. As expected, the prediction errors decrease exponentially as the look-ahead distance decreases. The relatively small prediction errors suggest that the proposed tactile terrain prediction method is a viable low-cost option for use in autonomous and tele-operated ground vehicles.

INTRODUCTION

Unmanned ground vehicles (UGV's) have demonstrated an ability to support in theater operations including missions such as reconnaissance, surveillance, supply transport, and protection, as well as neutralizing improvised explosive devices [1]. Future operational needs call for increased levels of autonomy and perception-based adaptive tactical behavior. Current autonomous and tele-operated ground vehicles typically employ overly conservative path planning and driving strategies to ensure safe operation over challenging and uncertain terrain. UGV platforms are expected to achieve significant increases in performance through an improved understanding of local terrain characteristics [1], thereby enabling the vehicle to optimally adjust driving strategies and path planning to maximize performance.

Lidar or ladar measurement systems have been used on UGV's to provide preview information of the terrain topology in the immediate path of the vehicle [2-4]. Vision-based measurement systems are being used more frequently to provide similar terrain preview information to either replace or supplement lidar data [5-8]. Unfortunately, both of these measurement solutions often provide erroneous terrain measurements for common environmental conditions such as wet or snow-covered roads, shadows, superficial ground coverings, and deceptive surface textures [9].

Tactile feedback is an emerging solution that can be considered as either an alternative or a supplement to existing terrain measurement systems, depending on the application needs. Although a variety of strategies have been developed, tactile feedback typically utilizes an array of low-cost sensors attached to the moving UGV to predict the macro-scale features of local terrain in the immediate path of the vehicle [10-11]. Tactile feedback uses past history to extrapolate future terrain profile information.

The objective of this paper is to document a preliminary evaluation of a proprietary tactile feedback method for terrain profile prediction. This tactile terrain prediction method was implemented on a 6-DOF human-in-the-loop (HIL) driving simulator, and was subsequently evaluated on four unique test courses under a variety of operating conditions. Experimental prediction errors at look-ahead preview distances up to 25m are presented.

TACTILE TERRAIN MEASUREMENTS

Figure 1 depicts a UGV traveling along a path *s* through a Cartesian coordinate system defined by coordinates (*x, y, z*). Path planning algorithms require information about the terrain surface topology immediately in front of the vehicle as indicated by the green triangular patch in figure 1. The extent of the look-ahead preview distance will ultimately depend on the maximum speed that the UGV will be traveling, as well as the computational speed of the path-planning algorithm; however, this distance is always finite.

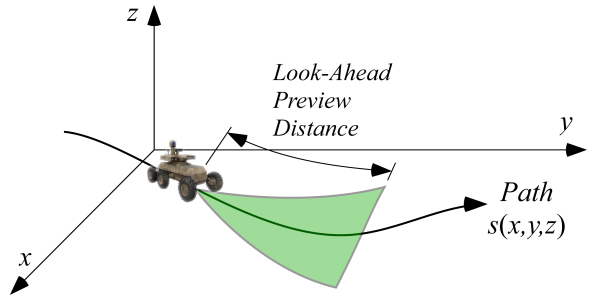

Figure 1. Unmanned ground vehicle with triangular look-ahead terrain preview region

The tactile terrain prediction algorithm evaluated in this effort is represented by the block diagram of figure 2. Relatively low-cost on-board sensors such as accelerometers and inclinometers [11] mounted on the UGV provide tactile measurements of the terrain topology at the current location. These measurements are combined with a finite and immediate past history of similar terrain topology data as indicated in figure 2. This historical data is then used to predict the low wave-number features of the terrain in a finite look-ahead preview region using an extrapolation technique. The explicit details of this algorithm are restricted from publication, pending a patent filing.

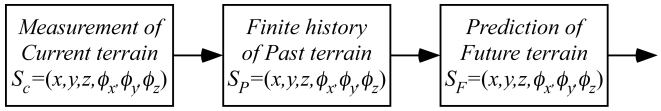

Figure 2. Unmanned ground vehicle with triangular look-ahead terrain preview region

As should be expected, the tactile feedback approach does not have the ability to predict obstacles, and the prediction error is expected to increase as the look-ahead preview distance increases. Even with this known limitation, predictions of terrain topology based on tactile feedback can be fused with lidar or vision-based data to overcome the measurement deficiencies, and ultimately improve the overall accuracy for path-planning and autonomous navigation. Ideally for UGVs on rough terrain, tactile terrain prediction algorithms will enable the processing of lidar and/or vision data to focus on obstacle detection through data fusion with the predicted terrain profile.

HIL EXPERIMENTAL TEST PLATFORM

In order to evaluate the performance of the proprietary tactile terrain prediction method over a range of terrain courses, vehicles, drivers, and operational conditions, the prediction system was integrated with a 6-DOF human-in-the-loop (HIL) driving simulator as shown in figure 3.

In this HIL driving simulator, the steering, throttle, brake, and gear selection commands from the human driver are processed through a natural cockpit interface. These commands are applied as inputs to one of many possible vehicle dynamics simulation models, which interact with one of many possible terrain maps to provide visual, audio, 6-DOF motion, and tactile feedback to the driver. Within the virtual environment, all pertinent signals of interest were available for predicting the look-ahead terrain profile. In order to more accurately represent a real vehicle on actual terrain, apriori knowledge of the terrain profile was not used in this study.

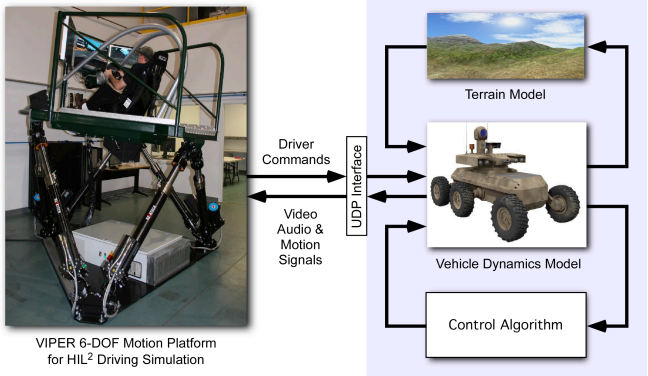

Figure 3. 6-DOF Driving Simulator used for experimental HIL testing of tactile terrain prediction algorithm

EVALUATION CASE STUDIES

Four test courses were selected to evaluate the tactile terrain prediction method. The first three courses were paved tracks: (A) Road America, in Elkhart Lake, Wisconsin; (B) Virginia International Raceway, in Alton, Virginia; and (C) Zandvoort, in the Netherlands. The fourth course was a mixture of off-road terrain and rough pavement: (D) Pikes Peak, in Colorado Springs, Colorado. These courses and the corresponding test conditions are summarized in table 1.

Table 1. Summary of courses and drivers used in case study.

Case	Course	Driver	Course Description
A	Road America	Human	6604 m course length 48 m elevation change
B	Virginia Int'l Raceway	AI	6359 m course length 46 m elevation change
C	Zandvoort	AI	4427 m course length 9 m elevation change
D	Pikes Peak	Human	11630 m course length 914 m elevation change

Figure 4 is a plot of overhead views for each of the four test courses where the *x*–axis represents the easting direction in meters, and the *y*–axis represents the northing direction in meters. Waypoint markers have been included on each of the subplots in figure 4. For courses A, B, and C, the waypoint spacing is 1000 meters, and for course D, the waypoint spacing is 2000 meters. The waypoint markers with subscript-1 represent the starting point for each test.

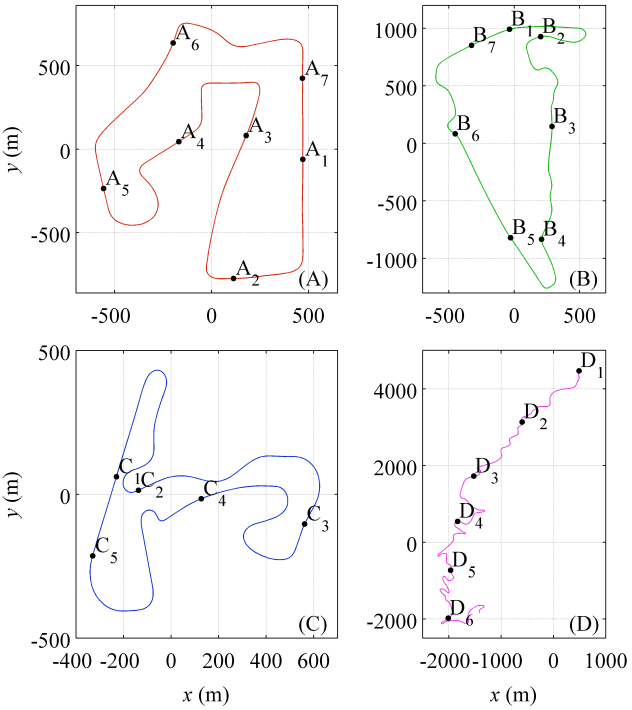

Figure 4. Test courses: (A) Road America, (B) Virginia International Raceway, (C) Zandvoort, (D) Pikes Peak.

From table 1, notice that courses A and B are similar in length and elevation change. Course C was the shortest with the least amount of elevation change, and course D was the longest with the largest elevation change. Courses A and D were driven with a human driver in the loop to simulate a tele-operated ground vehicle, and courses B and C were driven with an artificial intelligence (AI) driver to simulate a fully autonomous ground vehicle. During the testing, both a human and an AI driver were independently allowed to drive on the same test course. No significant differences were observed between the prediction errors for the fully autonomous and the tele-operated cases. This is a strong testament to the robustness of the proprietary tactile terrain prediction algorithm to driver style and speed. In all test cases, the ground vehicle speeds ranged from zero to 80 kilometers/hour.

TERRAIN PREDICTION RESULTS

The results of each of the four test cases are presented in figures 5, 6, 7, and 8 respectively. Each figure contains four subplots, and each subplot shares a common horizontal axis, which is the path position *s* in meters. The topmost subplot in each figure is the elevation profile *z* in meters, as a function of path position. The corresponding waypoint markers are included on the elevation profiles to enable cross-referencing with figure 4. The second subplot from the top of each results figure is the localized *Grade* of the terrain profile expressed with units of degrees. The grade is a measure of the spatial rate of change of elevation along the path. The third subplot from the top of each figure is the localized *Grade Rate*, which is the spatial rate of change of the grade along the path. The units of grade rate are expressed here as degrees/meter; however, the actual units are not critical to the analysis as will be shown below. The grade and grade rate subplots in each results figure are not directly part of the tactile terrain profile prediction method. They are merely included here for analysis purposes.

The bottom subplot in each results figure contains the most important data. These subplots indicate the *Prediction Error*, expressed in meters, at five equally spaced look-ahead locations along the path in front of the vehicle. Note that the tactile terrain prediction algorithm is actually designed to predict the profile over a continuum of points in the immediate path of the vehicle; however, only a discrete set of look-ahead points at five meter increments are presented here for brevity.

One segment of terrain between waypoints A_5 and A_6 in figure 5 has a very flat elevation profile. As expected in this region, the prediction error is nearly zero up to a 25m look-ahead distance. The prediction error in figure 5, and all subsequent results figures, can be characterized as zero-mean with occasional oscillatory bursts.

As indicated in figure 4, each test course has multiple turns in both directions so steering was a logical initial choice for the root cause of the prediction error bursting. After direct comparison of the prediction error bursting with steering angle, no correlation could be found. This led to an analysis of grade and grade rate.

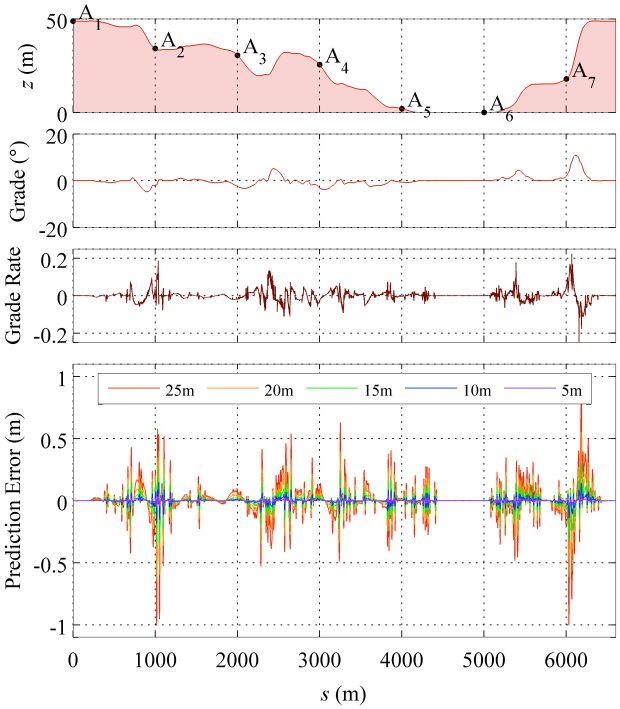

Figure 5. Terrain prediction errors on Road Atlanta course.

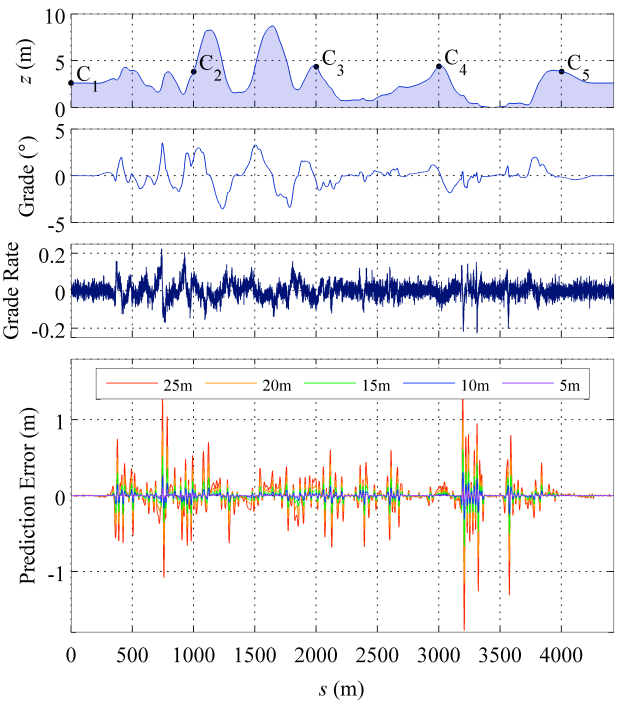

Figure 7. Terrain prediction errors on Zandvoort course.

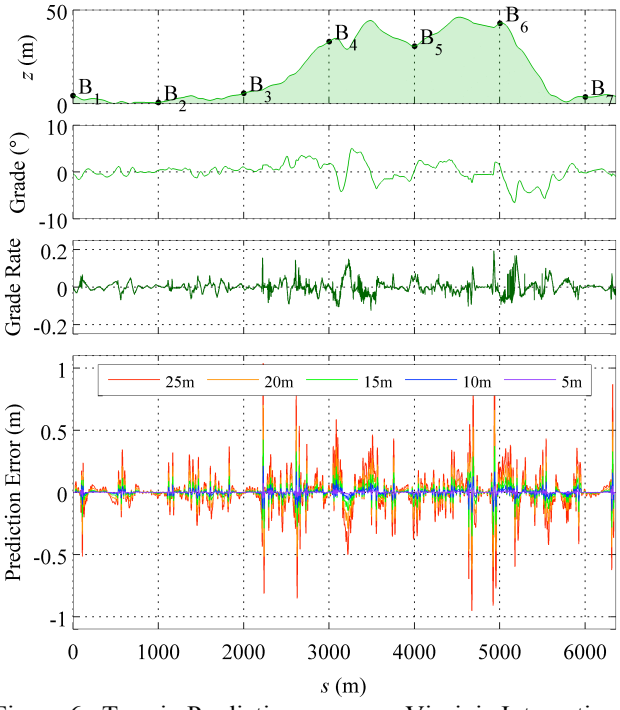

Figure 6. Terrain Prediction errors on Virginia International Raceway course.

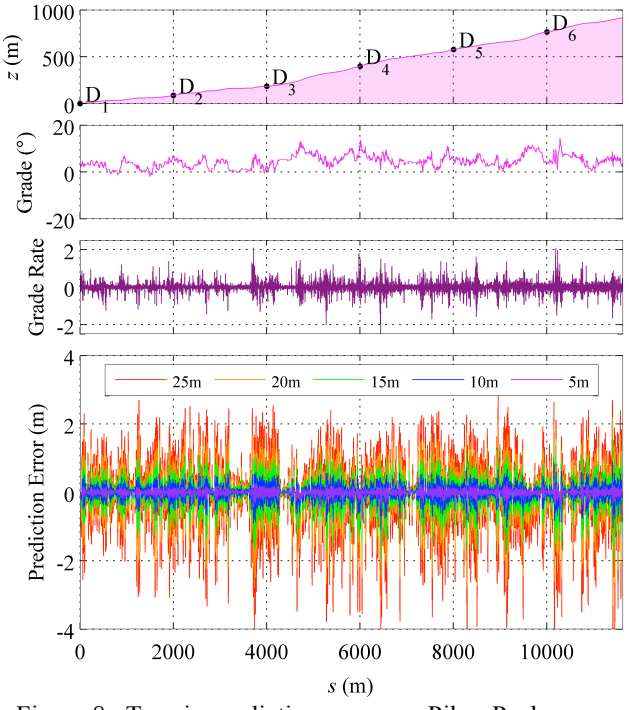

Figure 8. Terrain prediction errors on Pikes Peak course.

In order to quantify the performance of the tactile terrain profile estimation method, the worst case values of the prediction errors were extracted from the data in figures 5, 6, 7, and 8. Table 2 contains a summary of the peak prediction errors. Since all four of the figures above clearly indicate that the peak errors occur relatively infrequently, the rms prediction errors were also computed, and are presented in table 3.

Table 2: Peak Prediction Errors (all units are in meters)

Look-Ahead	A	B	C	D
5 m	0.063	0.076	0.103	0.483
10 m	0.184	0.213	0.314	1.098
15 m	0.376	0.422	0.671	2.072
20 m	0.650	0.701	1.158	3.312
25 m	1.006	1.037	1.775	4.863

Table 3: RMS Prediction Errors (all units are in meters)

Look-Ahead	A	B	C	D
5 m	0.007	0.009	0.013	0.086
10 m	0.022	0.026	0.039	0.220
15 m	0.048	0.056	0.082	0.422
20 m	0.087	0.101	0.143	0.696
25 m	0.139	0.161	0.220	1.036

Closer inspection of figures 5, 6, 7, and 8 indicates that localized spikes in the prediction errors are highly correlated to corresponding spikes in the grade rate. This means that the grade rate, which can effectively be measured using tactile feedback data, provides a real-time mechanism for predicting the accuracy of the look-ahead data. Ultimately, this means that instantaneous spikes in the grade rate will cause the look-ahead prediction errors to increase and then rapidly return to nominal levels.

For each test case, the results from both tables 2 and 3 also indicate a common trend that the prediction error increases approximately exponentially with look-ahead distance. This trend is completely expected considering that the prediction method is an extrapolation based on current and past data.

Table 4 summarizes the non-dimensional crest factor data for each of the prediction error curves in figures 5-8. The crest factor is defined to be the ratio of the peak error to the rms error. Notice from table 4 that courses A, B, and C all have very similar prediction error crest factors, which are relatively high values. Track D has a lower prediction error crest factor, indicating that the rms error is closer to the peak error; however, a crest factor of 5.0 is still relatively high. It is also interesting to note that in courses A, B, and D, the prediction error crest factor decreases as the look-ahead distance increases, which is expected. The smallest prediction error crest factors for case C occur at 5m and 10m.

Table 4: Crest Factor analysis (non-dimensional)

Look-Ahead	A	B	C	D
5 m	9.00	8.44	7.92	5.62
10 m	8.36	8.19	8.05	4.99
15 m	7.83	7.54	8.18	4.91
20 m	7.47	6.94	8.10	4.76
25 m	7.24	6.44	8.07	4.69

When the tactile terrain prediction algorithm is used to supplement existing measurement systems for improving the accuracy of path planning, both the localized grade rate information and the known exponential error trend can be exploited to determine error covariances for Kalman-based data fusion. Similar to the limitation of all tactile feedback prediction algorithms, unfortunately, the grade rate information cannot be used to predict obstacles.

Although not shown in this paper, the same tactile feedback method used for predicting the terrain profile along the vehicle path can also be used for predicting the terrain roll angle along the path. This lateral profile information when combined with the longitudinal profile information provides a more complete picture of the look-ahead terrain.

CONCLUSIONS

A proprietary tactile terrain prediction method was integrated into a HIL driving simulator for evaluation on four unique test courses. Two of the courses were driven with human drivers to simulate tele-operation of a UGV, and the other two courses were driven with a fully autonomous UGV. As expected, the prediction errors decrease as the look-ahead distance decreases, and the error tends to follow an exponential behavior. In all cases up to 25m look-ahead distance, the prediction errors can be characterized as having a relatively high crest factor ranging from a 4.69 to 9.0, which means that the peak errors occur infrequently. The peak errors are correlated to the grade rate and therefore can be accommodated in practice.

ACKNOWLEDGEMENT

The author wishes to thank the Institute for Advanced Learning and Research for their support.

REFERENCES

[1] Clapper, J.R., Young, J.J., Cartwright, J.E., Grimes, J.G., Payton, S.C., Stackley, S.J., and Popps, D., "FY2009 - 2034 Unmanned Systems Integrated Roadmap," *DOD Memorandum for Secretaries of the Military Departments*, 2nd Ed., April, 2009

[2] Manduchi, R., Castano, A., Taluker, A., and Matthies, L., "Obstacle Detection and Terrain Classification for Autonomous Off-road Navigation," *Robotics and Automation*, vol 18, pp 81-102, 2005

[3] Hebert, M., and Vandapel, N., "Terrain Classification Techniques from Ladar Data for Autonomous Navigation," *Collaborative Technology Alliances Conference*, 2003

[4] Vandapel, N., Huber, D., Kapuria, A., and Hebert, M., "Natural Terrain Classification using 3-d Ladar Data," *IEEE Int. Conference on Robotics and Automation*, New Orleans, USA, 2004

[5] Bellutta, P., Manduchi, L., Matthies, K., Owens, K., and Rankin, A. "Terrain Perception for Demo III," *IEEE Intelligent Vehicles Symposium*, Dearborn, USA, 2000

[6] Castano, R., Manduchi, L., and Fox, J., "Classification Experiments on Real-Word Textures," *Workshop on Emp. Eval. in Computer Vision*, Kauai, USA, 2001

[7] Seraji, H., "Traversability Index: A New Concept for Planetary Rover," *IEEE Int. Conference on Robotics and Automation*, Detroit, USA, 1999

[8] Poppingga, J., Birk, A., and Pathak, K., "Hough Based Terrain Classification for Realtime Detection of Drivable Ground," *Journal of Field Robotics,* vol 25, no 1, pp 67-88, 2008

[9] Guo, Y., Song, A., Bao, J., Tang, H., and Cui, J., "A Combination of Terrain Prediction and Correction for Search and Rescue Robot Autonomous Navigation," Int. J. of Advanced Robotic Systems, vol 6, no 3, pp 207-214, 2009.

[10] Iagnemma, K., and Dubowsky, S., "Terrain estimation for high-speed rough-terrain autonomous vehicle navigation," *Proc. of SPIE*, vol 4715, pp 256-266, 2002.

[11] Park, J.B., Lee, J.H., and Lee, B.H., "Online Turnover-Free Control for a Mobile Agent with a Terrain Prediction Sensor," *J. of Field Robotics*, vol 23, no 1, pp 59-77, 2006.